Diffractive limited acoustic field of an apodized ultrasound transducer

Vera L. S. Nantes Button[a], Eduardo Tavares Costa[b], Joaquim M. Maia[c] ,Ricardo G. Dantas[d]

Departamento de Engenharia Biomédica, Faculdade de Engenharia Elétrica e de Computação e Centro de Engenharia Biomédica, Universidade Estadual de Campinas / Campinas, SP, Brazil.

ABSTRACT

The diffraction in the acoustic field of an ultrasound transducer can be modeled as the result of the interference of edge and plane waves generated from the periphery and the center of the piezoelectric element, respectively. Our objective in developing ultrasound transducers with apodized piezoelectric ceramic discs was to generate acoustical fields with reduced edge waves interference. Transducers were built with apodized ceramic discs (polarized more intensively in the central region than in the edges) and their mapped acoustic fields showed a distinct pattern when compared to those of conventional transducers. A polynomial equation describing the nonlinear poling field intensity, was used with the Rayleigh equation to simulate the nonuniform vibration amplitude distribution generated by the apodized transducers. Simulated acoustic fields were compared to experimental field mappings. The results of simulations and experimental tests showed reduction in the lateral spreading of acoustic fields produced by apodized transducers, compared to those produced by conventional transducers. The reduced presence of the lateral lobes in the apodized acoustic field is due to the minimized vibration of the disc periphery. The numerical and experimental results were in good agreement and showed that it was possible to reduce acoustic field diffraction through nonlinear polarization of the piezoelectric element.

Keywords: apodization; ultrasound transducer; piezoelectric ceramic; acoustical field, diffraction; interference.

1. INTRODUCTION

The pulsed field of a circular ultrasonic transducer can be described by the interaction of its two components: plane waves, radiated from the whole face of the transducer, and edge waves, radiated from its edge. The diffraction in the acoustic field can be modeled as the result of the interference of edge waves and plane waves, and defines the near field (characterized by maxima and minima) and far field regions of the acoustic field[1,2].

Transducer apodization has been studied intensively with researchers looking for ultrasound fields without diffraction in the near field of the transducers or ultrasound fields with special characteristics like Gaussian fields[3] or X-fields[4]. The apodization term is used in the literature to describe the acoustic field formatting. In order to reduce diffraction effects, several methods are reported, like the use of lenses[5], the use of distinct electrical voltages pulses to selectively excite parts of the piezoelectric element(s)[6], and the use of non-linear polarized piezoelectric element(s)[7]. It is highly desirable to obtain ultrasound transducers with good lateral resolution over a large depth of field and without lateral lobes, if we intend to obtain medical images and/or perform materials testing.

We have been studying acoustic field apodization for several years with the objective of developing ultrasound transducers with apodized piezoelectric ceramic discs. In our work we produced apodized piezoelectric ceramic discs (single element, 1mm thick, 6.35mm radius) by the use of non-linear electrical poling field, in a way that the ferroelectric dipoles in the central region of the disc are strongly oriented by the poling field, and the dipoles in the edge of the disc are less intensely oriented. We investigated the poling process of piezoelectric ceramic discs with various electrode formats to achieve an ideal electrical field intensity profile, that would result in a ceramic disc that vibrates more intensely in the central region than in its periphery. To define the ideal poling profile we performed finite element method simulations. Then we apodized ceramic discs and constructed the transducers. The apodization process and the performed tests were described in previous work [8].

Correspondence : e-mail: [a]vera@deb.fee.unicamp.br; [b]educosta@ceb.unicamp.br; [c]joaquim@ceb.unicamp.br; [d]grossi@ceb.unicamp.br.

In *Medical Imaging 2000: Ultrasonic Imaging and Signal Processing*, K. Kirk Shung, Michael F. Insana, Editors, Proceedings of SPIE Vol. 3982 (2000) • 1605-7422/00/$15.00

In this work we have used the ideal poling profile, defined after the FEM simulations, to modify the velocity potential distribution of the ceramic disc undergoing sinusoidal movement and used the Rayleigh equation to simulate the ultrasound field irradiated to an ideal fluid. We have introduced the apodization effect in the field calculation, in a manner to minimize the contribution of the peripheral region of the vibrating piezoelectric disc.

2. METHODOLOGY AND RESULTS

2.1. FEM simulations of non-linear piezoelectric ceramic discs polarization

Finite element method (FEM) simulations were performed to preview the profile intensity of the poling field of piezoelectric ceramic discs, 1mm thick and 12.7mm diameter, when using spherical electrodes of different radius. Some results are shown in figure 1.

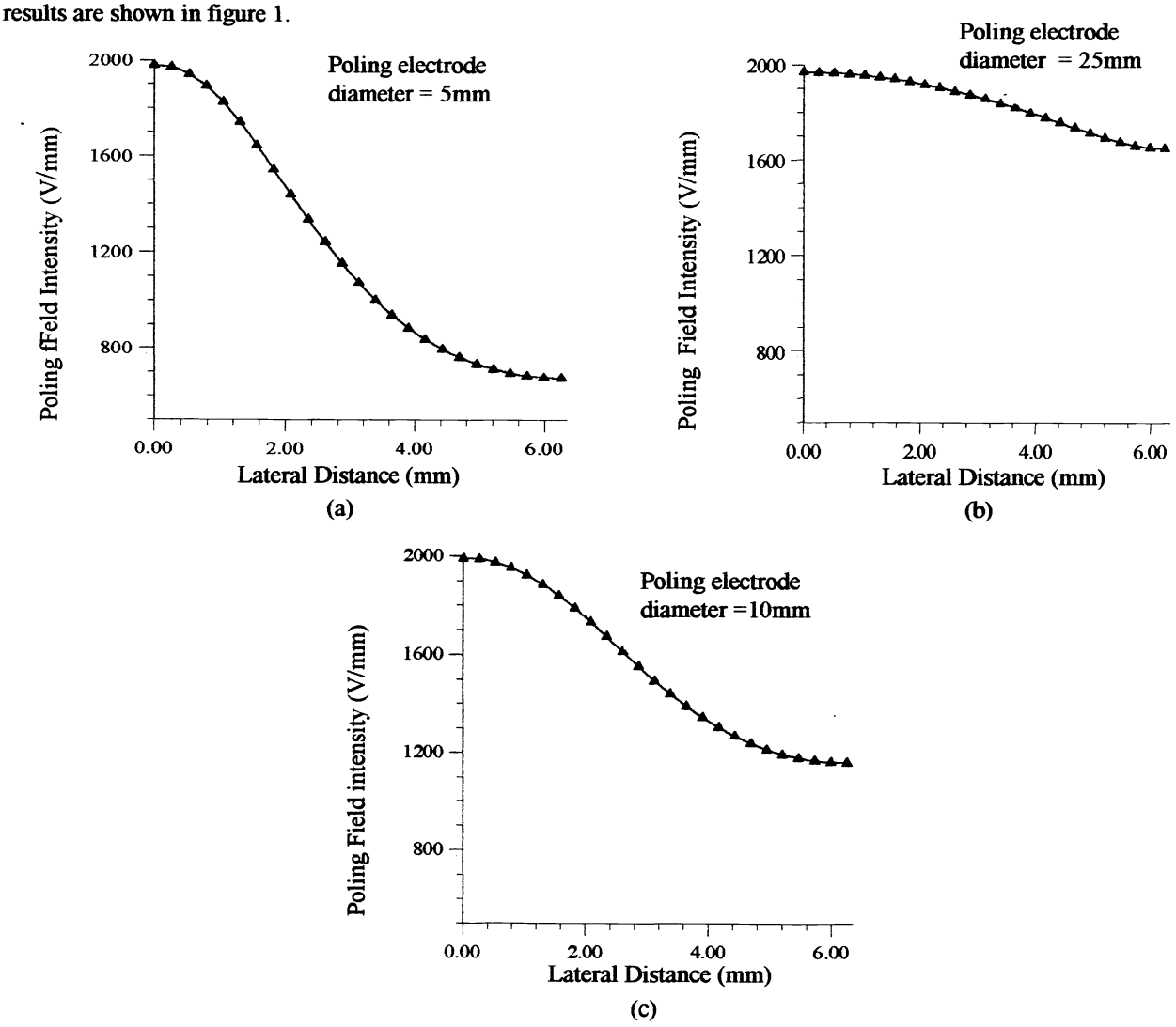

Figure 1. Electrical intensity profile of the non-linear poling field produced in a piezoelectric ceramic disc (1mm thick and 12.7mm diameter) by spherical poling electrodes of 5mm (a), 25mm (b) and 10mm (c) diameter. Lateral distance = 0 coincides with the center of the ceramic disc.

A spherical electrode with 10mm diameter was chosen to substitute the conventional surface deposited electrode. A 2kV voltage was applied to the spherical electrode, placed in the center of the disc face that had the original electrode removed, and the other face (deposited electrode) was grounded. Poling electrodes with diameters greater than 10mm would produce an electrical poling field with almost the same intensity all over the ceramic (figure 1 (b)), and poling electrodes with diameter smaller than 10mm would polarize just a small part of the ceramic disc (figure 1(a)), resulting in weak acoustical pulses. The FEM simulations also provided the graphical representation of the distribution of electrical dipoles along the ceramic disc radius. In figure 2 we can see that electrical dipoles are more concentrated in the central region of the disc and that their intensities are greater than those of the disc edge.

The FEM simulations allowed us to determine a fifth degree polynomial equation that describes the nonlinear poling electric field intensity inside the ceramic disc, as a function of its radius. This polynomial equation was used, in our present work, with the Rayleigh equation to simulate the acoustic field produced by the non-uniform vibration amplitude distribution of the apodized transducers. We have performed simulations using Matlab (Mathworks Inc.) and C language programs of apodized and non-apodized acoustic fields and compared them to the experimental field mappings.

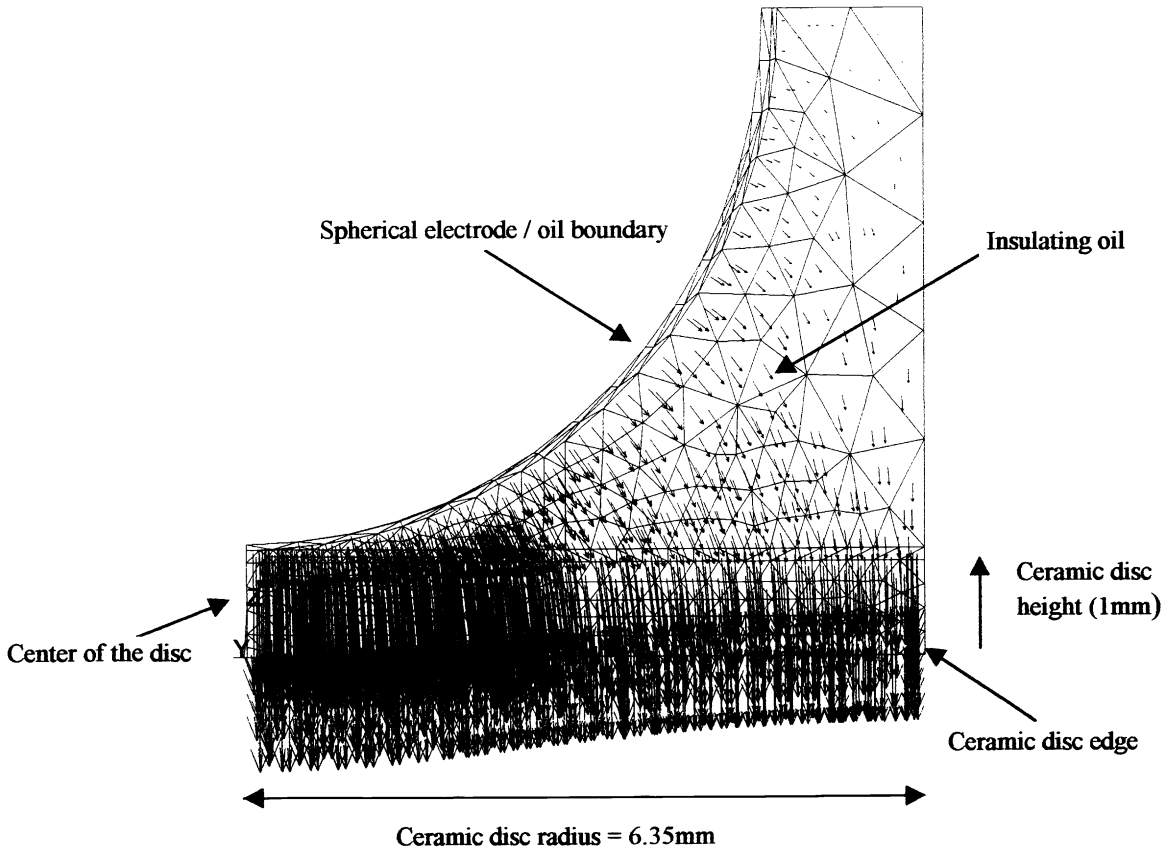

Figure 2. Distribution of the electrical dipoles along the ceramic disc radius, and in the insulating oil, while the disc is polarized by a spherical electrode (10mm diameter) connected to a 2kV electrical voltage. The bottom face of the disc is grounded. The intensity modulus of each vector is proportional to its size.

2.2. Experimental results

Ultrasound transducers were built with commercial, conventionally polarized, ceramic discs, and with apodized ceramic discs. The apodized discs were polarized with a 10mm diameter spherical electrode and were expected to vibrate more intensively in their central region than in their edges, producing ultrasound fields with less diffraction effects.

The resultant acoustic fields of apodized and non-apodized transducers were mapped in a water tank, using a punctual hydrophone, and showed that it was possible to reduce the diffraction interference by modifying the polarization of the piezoelectric ceramic discs. Figure 3 shows the field mapped along the acoustical axis (Y axis) for two transducers: one constructed with commercial ceramic (b) and one constructed with the apodized ceramic (a). Figure 4 shows the acoustical field mapped on XY plan for these transducers.

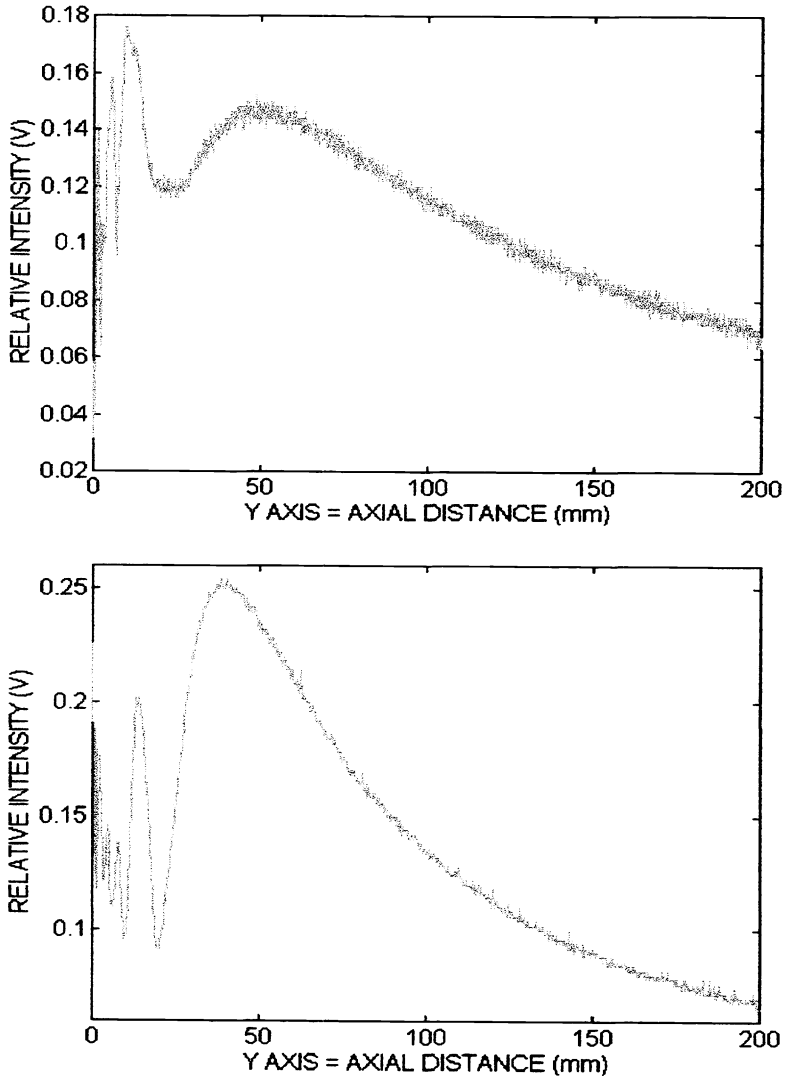

Figure 3. Field mapped over the acoustic axis (Y) for two transducers: one constructed with commercial ceramic (b) and one constructed with apodized ceramic (a).

Comparing the ultrasound fields mapped for both transducers, the apodized transducer showed an ultrasound field with less side lobes and larger depth of field that is evident in the –3dB and –6dB contour plots of the field .

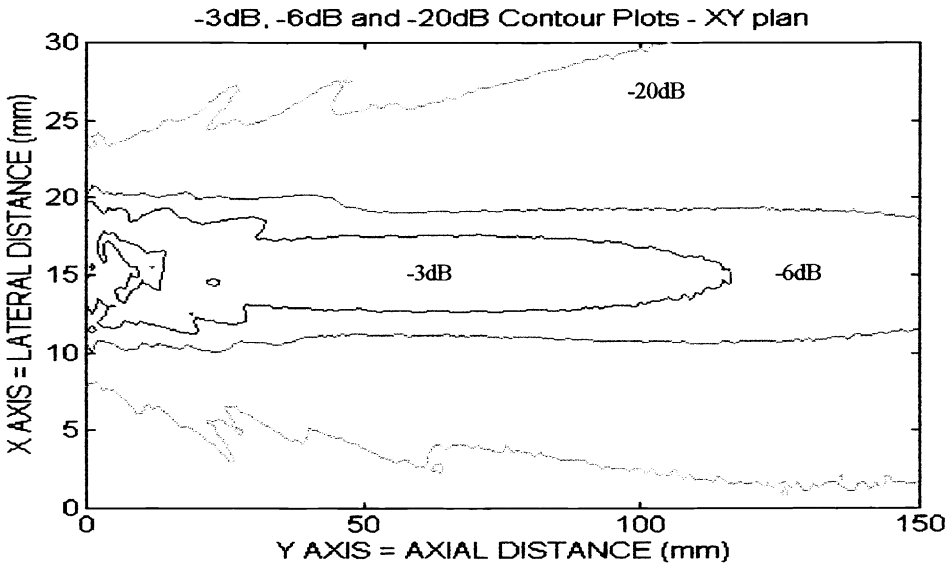

(a)

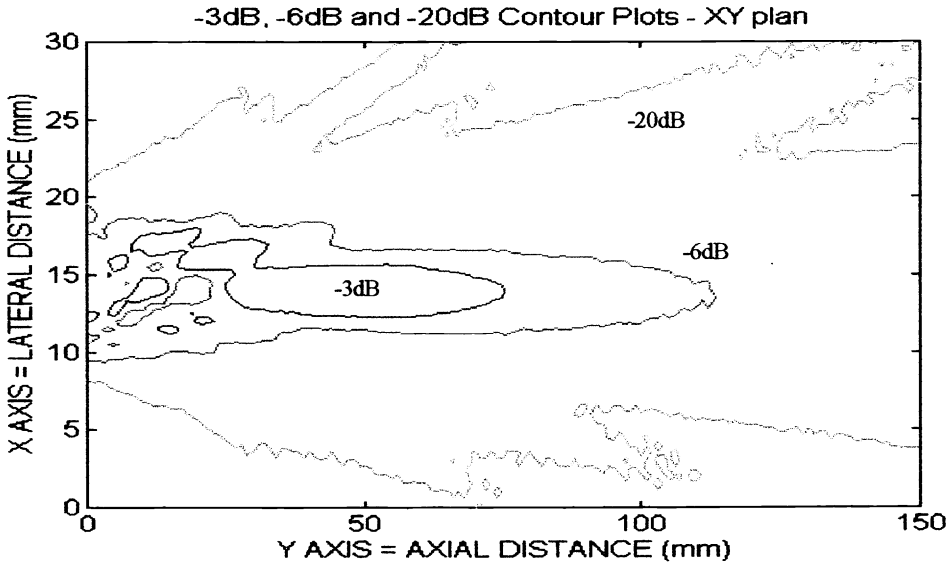

(b)

Figure 4. Contour plots (-3dB, -6dB and –20dB) of the acoustic fields mapped on XY plan for two transducers: one constructed with commercial ceramic (b) and one constructed with apodized ceramic (a).

2.3. Acoustical field simulations

The radiated field of a planar vibrating source (uniform motion) in an infinite rigid baffle can be expressed by the Rayleigh[9] surface integral:

$$\phi = \int_S \frac{v(t - R/c)}{2\pi R} dS \tag{1}$$

where: $\phi =$ velocity potential
$v =$ velocity of the piston
$R =$ distance from the field point P to a surface element dS
$c =$ propagation velocity of the sound

This equation represents the velocity potential in a field point P, as the sum of the contributions of all dS surface piston elements, radiating into an ideal fluid (isotropic, homogeneous and loss-less).

The equation to calculate the pressure of sound in the field point P, in a fluid of density ρ, can be expressed as:

$$P = \rho \frac{\partial \phi}{\partial t} \tag{2}$$

The function velocity of the piston can be expressed as the convolution of the velocity of the piston and the delta function:

$$v(t - R/c) = \int v(\tau)\delta(t - R/c - \tau)d\tau = v(t) * \delta(t - R/c) \tag{3}$$

Equations (1) and (2) can be rewritten as:

$$\phi(R,t) = v(t) * \phi_i(R,t) \tag{4}$$

and

$$P(R,t) = v(t) * P_i(R,t) \tag{5}$$

where $\phi_i(R,t) = \int_S \frac{\delta(t - R/c)}{2\pi R} dS$, is the velocity potential impulse response, and

$P_i(R,t) = \rho \frac{\delta \phi_i(R,t)}{\delta t}$, is the pressure impulse response.

Equation (5) can also be expressed by:

$$P(R,t) = \rho \phi_i(R,t) * \frac{\delta v(t)}{\delta t} \tag{6}$$

Equation (6) allows the calculation of the acoustic pressure due to any arbitrary velocity function. For a sinusoidal excitation of the ultrasound transducer, the velocity of the piston is:

$$v(t) = V_0 sin(w_0 t) \tag{7}$$

To introduce the apodization effect in the transducer surface movement, we have multiplied V_0 by the normalized fifth degree polynomial equation obtained from the apodization FEM simulations, that describes the polarization electric field intensity profile inside the ceramic disc:

$$V_{apodized} = V_0\left(1 + 12.09 \cdot 10^{-3} r - 45.1 \cdot 10^{-3} r^2 + 33.8 \cdot 10^{-4} r^3 + 8.6 \cdot 10^{-4} r^4 - 9.05 \cdot 10^{-5} r^5\right) \tag{8}$$

where: $r =$ the distance from the center of the piezoelectric disc to dS
(minimum value = 0mm, and maximum = 6.35mm, radius of the disc).

$V_{apodized}$ is a function of r. Its maximum value is V_0 (center of the disc, $r = 0mm$) and it decreases toward the edge of the disc, where the polarization was less intense than in the center.

A different apodization pattern can be described by a gaussian profile, described by equation (9):

$$V_0 = \exp\left(-\left(\frac{r(i)}{a}\right)\right)^2, \quad i = 1,..n \tag{9}$$

where: $r(i) =$ distance from the center of the piezoelectric disc to a position i along the radial distance
$a =$ ceramic disc radius

Figure 5 shows the two distinct patterns of apodization, gaussian (equation(9)) and the one described by equation (8). Both are able to produce non-uniform velocity potential distribution over the ceramic disc, plotted as function its radius.

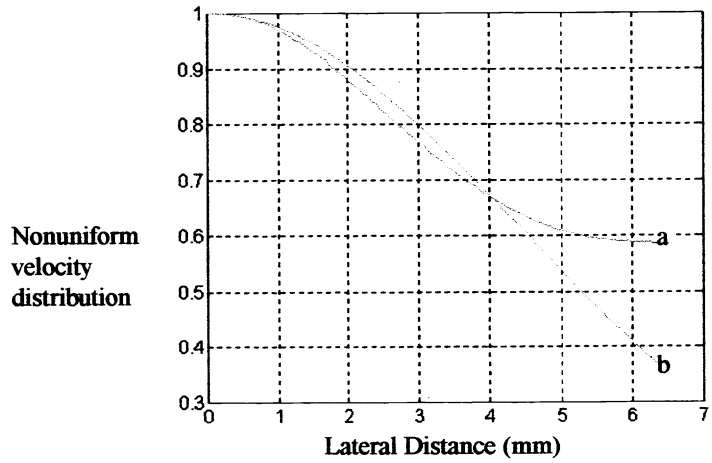

Figure 5. Non-uniform potential velocity profiles: the apodization produced by the spherical poling electrode (a)and the gaussian velocity distribution (b).

The polynomial apodization produces a non-uniform velocity potential similar to the gaussian profile from 0 to 4mm away from the center of the transducer. From this point on, the polynomial apodization maintains the poling electrical field intensity above 50% of the maximum amplitude, while the gaussian apodization decreases rapidly.
Figures 6 and 7 show the acoustic field simulations using equation (6), where $v(t)$ was replaced by equation (10):

$$v(t) = V_{apodized} sin(w_0 t) \tag{10}$$

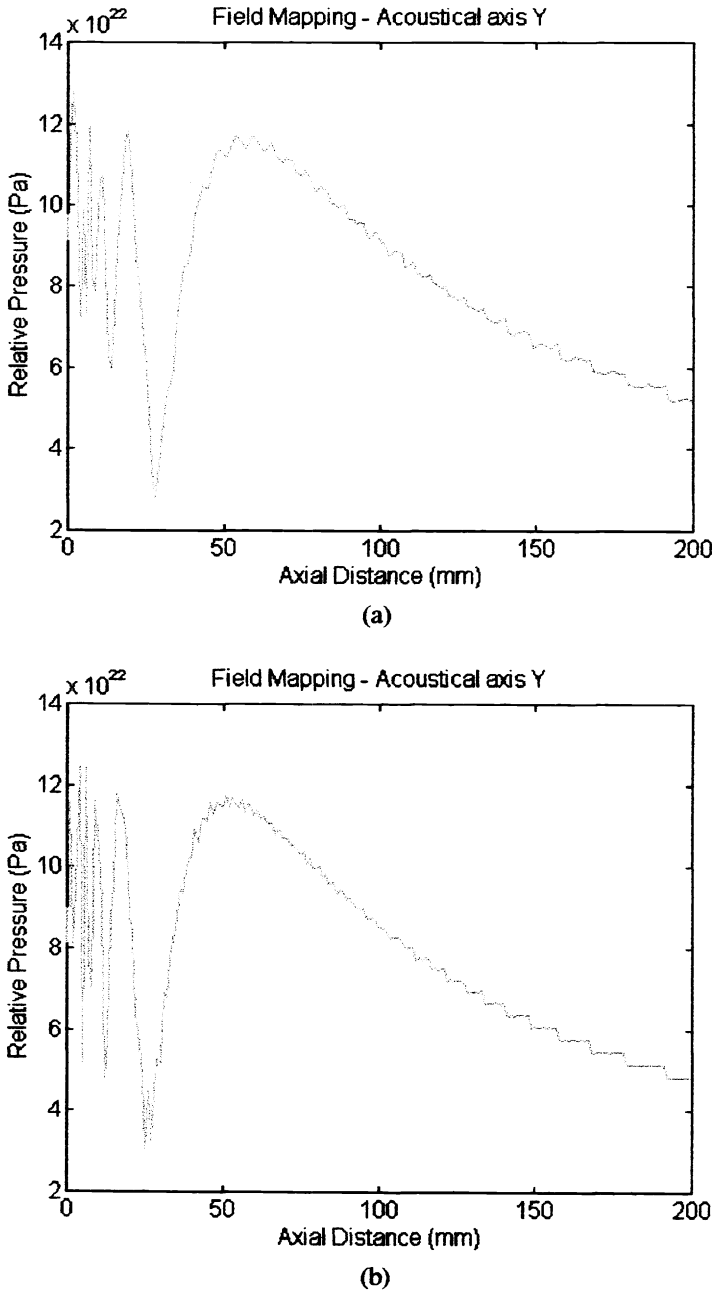

Figure 6. Simulated acoustic fields over the acoustical axis (Y) for two transducers: one with commercial ceramic (b) and one with apodized ceramic (a).

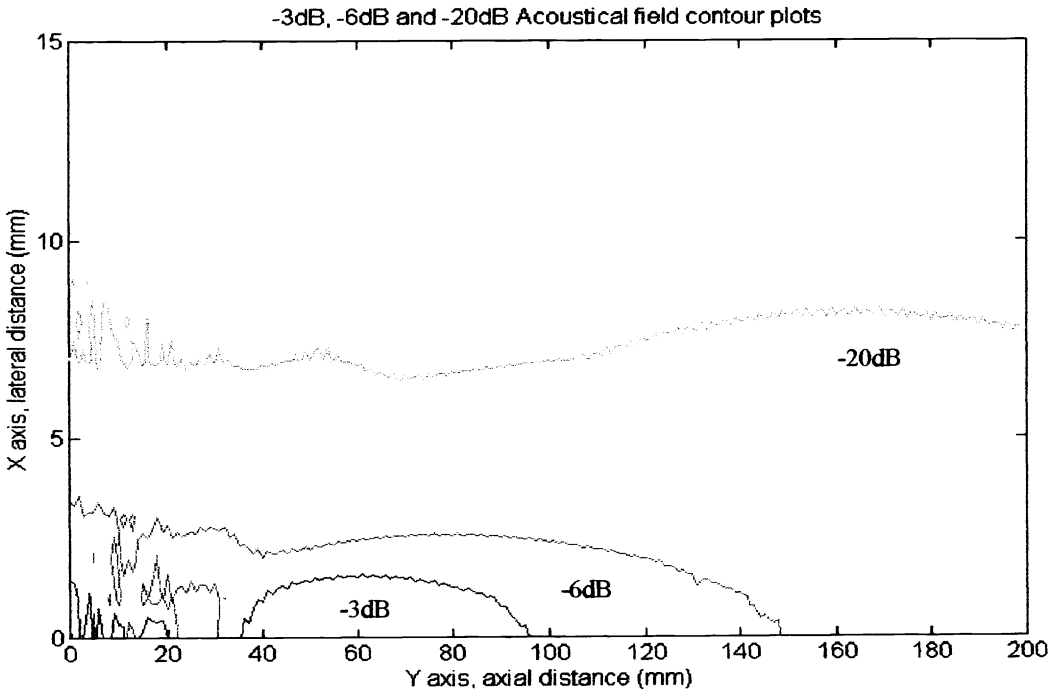

(a)

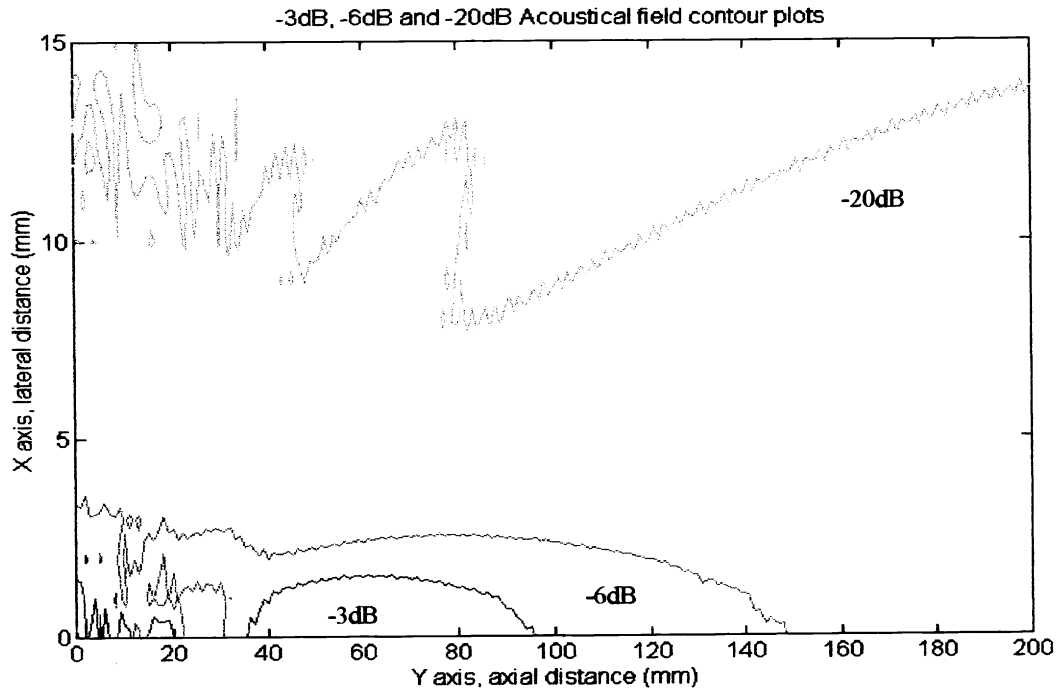

(b)

Figure 7. Contour plots (-3dB, -6dB and –20dB) of the acoustic fields (XY plan) simulated for two transducers: one with conventionally polarized ceramic (b) and one with apodized ceramic (a).

3. DISCUSSION AND CONCLUSION

The simulations showed a reduction in the lateral spreading of acoustical fields produced by the apodized transducers, compared to those produced by conventional transducers. The same effect was also verified in the experimental tests. The reduced presence of the lateral lobes in the apodized acoustical field is due to the minimized vibration of the periphery of the apodized ceramic disc that reduced the edge wave components.

The larger depth of field showed in the experimental field mappings of apodized transducers was not predicted by the acoustical field simulations when we used the convolution method. In our opinion, this is due to our model that do not incorporated the movement restrictions of the edge of the ceramic disc, inherent to the real transducer. It also did not account for the backing element of the real transducer.

The numerical and experimental results performed with one element transducers were in good agreement and showed that it is possible to reduce the diffraction on acoustic fields, through the nonlinear polarization of the piezoelectric element. Further experiments with apodized transducers will be carried out in order to evaluate the apodization effect on the ultrasonic image quality.

ACKNOWLEGMENTS

We would like to thank FINEP for the financial support.

REFERENCES

1. P. R. Stepanishen, "Transient radiation from pistons in an infinite baffle", *J. Acoust. Soc. Am.*, **49**. pp. 1629-1638, 1971.
2 J. P. Weight, "Ultrasonic beam structures in fluid media", *J. Acoust. Soc. Am.*, **76**. pp. 1184-1191, 1984.
3. D. K. Hsu, F. J. Margetan, M. D. Hasselbuch, S. J. Wormley, M. S. Hughes and D. O Thompson, "Technique of non-uniform poling of piezoelectric element and fabrication of gaussian transducers", *IEEE Trans. UFCC*, **37**, pp. 404-410, 1990.
4. J-Yu Lu and J. F. Greenleaf, "Ultrasonic nondiffracting transducer for medical imaging", *IEEE Trans. UFFC*, **37**, pp. 438-447, 1990.
5. D. R. Dietz, "Apodized conical focusing for ultrasound imaging" , *IEEE Trans. Sonics and Ultrasonics*, **29**, pp. 128-138, 1982.
6. R. H. Brittain and J. P. Weigth, "Fabrication of non-uniformly excited wide-band ultrasonic transducers", *Ultrasonics*, **25**, pp. 100-106, 1987.
7. K. Kawabe, Y. Hara, K. Watanabe and T. Shimura, " An ultrasonic transducer apodized by polarization", in: *IEEE Ultrasonic Symposium*, 1990.
8. V. L. S. Nantes Button, E. T. Costa and J. M. Maia, "Apodization of piezoelectric ceramics for ultrasound transducers ", in *Ultrasound Transducers Engineering*, K. K. Shung, Ed., Proc. SPIE, **3664**, pp. 108-118, 1999.
9 Lord Rayleigh, *Theory of Sound*, Dover, New York, 1945.